Lascala
Erasmus Mundus Master

Weekly practice work at the ELI facility

Applications of attosecond pulses

Practice syllabus

2022 Fall semester

Contents

1. Goal of the practice and practice specific requirements

1.1. Purpose of the practice

The goal of the practice is to give an overview on the basic technologies involved in generation and applications of attosecond pulses. The students will get knowledge and practical training on research equipment that are used to characterize spectral, temporal and spatial properties of extreme-ultraviolet (XUV) radiation that is produced using high harmonic generation (HHG) in gases. The students will learn and implement themselves basic evaluation methods of raw data obtained with the above equipment.

1.2. Requirements of the practice

The “Applications of attosecond pulses” practice starts with an entry test based on “Entry/control questions” listed in the end of this document. Three questions will need to be answered in written form. Passing this test is a prerequisite for doing the practice.

After passing the entry test, the laboratory practice will start with description of the safety features of the laboratory and the HHG beamline. Attendance to the laboratory safety training is mandatory, and participation has to be certified by signing the corresponding attendance sheet.

Measurement report preparation requires software capable of basic image processing and custom function fitting. Suggested options are Python and Matlab, but any other software can be used.

It is required from the students to include intermediate calculations and evaluation-step results in the measurement report. This helps lecturers to identify mistakes during evaluation and correcting mistakes.

2. Introduction to high-order harmonic generation in gases and characterization of the produced radiation

2.1. The theoretical background of high-harmonic generation in gases

HHG in gases is the result of the interaction of a strong infrared (IR) laser light field with gas atoms (most frequently noble gases like krypton (Kr), argon (Ar), neon (Ne) or helium (He)). During this process, a broad spectrum of electromagnetic radiation is generated, with a spectrum extending from the ultraviolet to the XUV (or X-ray spectral range), with peaks centered at odd multiples of the original field frequency (the generating laser field central frequency), as shown in Figure 1 [1]. Compared to other ways, very important advantages of generating XUV light using this method is that it inherits properties of the generating laser beam, like coherence, beam-like propagation and short duration. For example, the XUV beam size in the gas target is typically two-times smaller than the focused IR beam size, and divergence of the two beams also have similar

relation. Thanks to symmetry properties of the process, currently this is the most reliable way to produce light pulses (or pulse trains) with duration in the sub-femtosecond regime.

Several properties of the generated radiation can be understood by the three-step model (or simple man's model) of HHG, which describes the interaction of a single atom with the intense laser field in three steps:

- First step: removal of an electron from its parent ion by tunnel ionization induced by the high intensity (typically in the range of 10^{13} – 10^{15} W/cm^2) laser field.
- Second step: acceleration of the free electron. The motion is governed by the electric field of the laser pulse. This step can be described by classical physics using Lorentz force and Newton equations.
- Third step: the electron can return to the ionic core in some circumstances, and can recombine with it with a certain probability. In the classical approach, the gained kinetic and the binding energy are converted into an energetic XUV photon.

One important result of the three-step model (even though it uses classical physics to describe a quantum process) that it can predict the highest photon energy generated (called cut-off, see Figure 1) very accurately as

$$E_{\text{cut-off}} = I_\text{p} + 3.2U_\text{p}, \tag{1}$$

where I_p is the ionization potential (or energy) of the target atom (14.00 eV for Kr, 15.76 eV for Ar**,** 21.56 eV for Ne, 24.58 eV for He), and U_p is the ponderomotive potential (or energy), which is the average kinetic energy of the electron doing the oscillating motion under the influence of the laser field given by

$$U_\text{p} = \frac{(eE_0)^2}{4m\omega_0^2}. \tag{2}$$

In the previous expression e is elementary charge, E_0 is the amplitude of the monochromatic electric field, m is the mass of electron and $\omega_0 = 2\pi c/\lambda_0$ is the angular frequency of the electric field (c being the speed of light in vacuum and λ_0 the corresponding wavelength – this latter being the central wavelength of the laser field in practical cases). In a practically more convenient form the ponderomotive energy in electronvolts can be calculated as

$$U_\text{p}[\text{eV}] = 9.33 \times 10^{-14} \times I_L[W/\text{cm}^2] \times \lambda_0^2[\mu\text{m}], \tag{3}$$

where in the square brackets the units of each physical quantity in the expression is highlighted to get a numerically correct result. Since in reality in the laboratory the laser beam interacts with an ensemble of atoms (a "macroscopic target") and not a single one (the "microscopic target"), the experimentally observable cut-off often differs from the prediction of this simple rule. Taking into account that different atoms will interact with different laser fields (consider the spatial distribution of the beam), the observable XUV radiation will be the sum of the XUV fields from these individual emitters. Therefore, apart from the cut-off, other properties of the measured

spectra are also altered by macroscopic effects, which is termed as phase-matching in the literature [1].

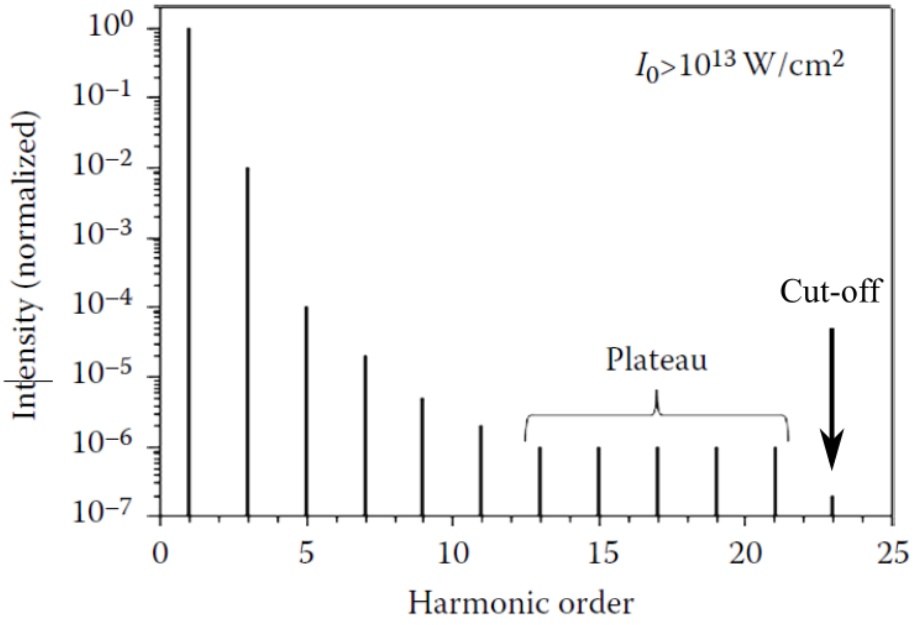

Figure 1. Schematic representation of a typical HHG spectrum. The spectrum (the photon flux or radiation intensity as a function of photon energy) consist of distinct harmonic peaks which are centered at odd multiples of the generating laser (angular) frequency. Image source: [1].

For high-order harmonics to be generated, a certain intensity of the laser field is necessary, primarily prescribed by the first step: for tunneling ionization to happen, a certain electric field strength is necessary to have enough force that can tackle the Coulomb force keeping the electron in the vicinity of the ionic core. These field strengths can be only achieved by focusing short laser pulses (durations in the femtosecond range). If we assume that the laser intensity profile $I_L(r)$ of the focused pulsed laser beam has a radial symmetry and a Gaussian spatial distribution of the form

$$I_L(r) = \exp(-2r^2/w^2), \tag{4}$$

the peak intensity of the field interacting with the gas target can be estimated as

$$I_0 = \frac{2\varepsilon_n}{\tau w^2 \pi}\sqrt{\frac{4\ln 2}{\pi}}, \tag{5}$$

where ε_n is the energy and τ is the intensity full-width-at-half-maximum (FWHM) duration of a single laser pulse. It is easy to see that reaching the required $I_0 > 10^{13}$ W/cm^2 intensity range even for femtosecond pulses with the available laser pulse energies a beam size in the micron range is necessary. So focusing of the input beam with radius w_{in} typically ranging between a few millimeters to a few centimeters is required, decreasing the spot size to the necessary value according to

$$w = \frac{\lambda}{\pi}\frac{f}{w_{\text{in}}}, \tag{6}$$

where *f* is the focal length of the optics used for focusing.

2.2. HHG with high average power laser beams – the HR GHHG Gas beamline of ELI ALPS

The High-repetition-rate laser-driven Gas-based High-order Harmonic Generation for Gas targets (HR GHHG Gas) beamline of the Extreme Light Infrastructure Attosecond Light Pulse Source (ELI ALPS) uses a high-average power laser, the HR-1 with 100 W of average power, to produce XUV radiation of attosecond pulse trains [2]. The schematic drawing of the laser and XUV beam paths are shown in Figure 2.

Due to the high average power of the laser beam, new considerations were necessary during design of the HR GHHG Gas beamline. In HHG beamlines it is a requirement that the generating IR laser beam is separated from the co-propagating, generated XUV beam, so a clean high-harmonic beam can be used for experiments. Since XUV radiation is absorbed in short distance basically by every material traverses – this is the reason for having HHG beamlines in vacuum chambers -, doing this separation of IR and XUV happens by putting a very thin (few hundreds of nanometer thick) metallic foil in the way of the beam (see the section in grey box in Figure 2 about "Filtering of generation IR from XUV"). These very thin metallic foils absorb the IR laser beam and have a transmission of few to few-tens of percent for XUV. See example transmission spectra for four different materials in Figure 3, often used for this purpose in HHG beamlines. Since the IR beam is to a big extent absorbed by these thin metallic foils, a high-power beam simply destroys them. A solution proposed in the 1990s was to use an annular laser beam, so block the central part of the beam before focusing it, which beam after the interaction point in the generation gas cell becomes again annular, and can be blocked by an annular block. Since often this type of filtering is not perfect, the two methods (annular generation beam and thin metallic foil) are combined, and this is the case for the HR GHHG Gas beamline as well (see the section in grey box in Figure 2 about "Filtering of generation IR from XUV"). The generation of the annular laser beam in the HR GHHG Gas beamline is done by using a mirror that has a hole in its middle (holey splitting mirror (HSM)), so only an annular part of the incoming laser beam is reflected (see an example in Figure 4(a)). The central part of the beam can be used for experiment requiring IR-XUV pump-probe capabilities (see the section in blue box in Figure 2 about "Splitting of the laser beam with holey splitting mirror (HSM)"). After generation, the (close-to) annular IR beam is blocked by the holey dump mirror (HDM), and only a minor portion is reaching the thin metallic filter.

One drawback of the annular generation beam is that part of the laser pulse energy is lost, since the central portion of the laser beam is not used for HHG. The smaller energy results in smaller peak intensity according to eq. (5), which gives a less broad spectrum as the cut-off law of eq. (1) suggests. The energy lost due to the annular splitting of the beam depends on the relative sizes of the circular hole on the HSM and the size of the incoming laser beam. This relation is not linear,

and the energy content in the hole as a function of incoming beam size is shown by Figure 4(b) for a fixed hole size (7 mm).

Since the XUV radiation produced using HHG is propagating in the form of a well-defined beam, just like the laser beam generating it, for successful experiments and detection the beam has to be steered in a way that it goes through a path during which it traverses necessary target areas (for example, the laser beam goes through the target gas cell) and in the end it reaches the sensitive surface of a detector (for example the multi-channel plate (MCP) of an XUV spectrometer). Since the generated XUV propagates collinearly with the generating IR field, the IR beam has to be aligned for having a successful experiment. For the experiments during this practice, this is done in two steps in the HR GHHG Gas beamline, indicated by yellow and green boxes in Figure 1 ("Alignment no. 1" and "Alignment no. 2"). Generally speaking, alignment of laser beams is a certain section of a beamline is done by adjusting the angle of two steering mirror mounts (see smaller boxes connected with continuous lines to the yellow and green description boxes in Figure 2) in a way that in two monitoring points the beam is centered on some references (see smaller boxes connected with dashed lines to the yellow and green description boxes in Figure 2). Since adjusting the angle of one mirror will affect the position of the beam at both monitoring points, this procedure has to be done in an iterative manner. For the iterative procedure to be convergent, the involved optical elements (the two mirrors and the two reference irises) have to follow each other in a certain order: first the two actuators followed by the two detectors. Aligning on references can be done by introducing a concentric diffraction pattern on the beam (for example by clipping the edges using an aperture), and aligning this diffraction pattern concentrically with the circular edge of an iris (see Figure 5 for examples). Since everything is under vacuum, mirrors steering the laser beam cannot be adjusted by hand, but by remotely controlled mirror mounts. Position of the beam with respect to the references can be monitored by cameras outside the vacuum chambers with properly designed imaging optics (lens system) to image the plane of the irises (see Figure 5).

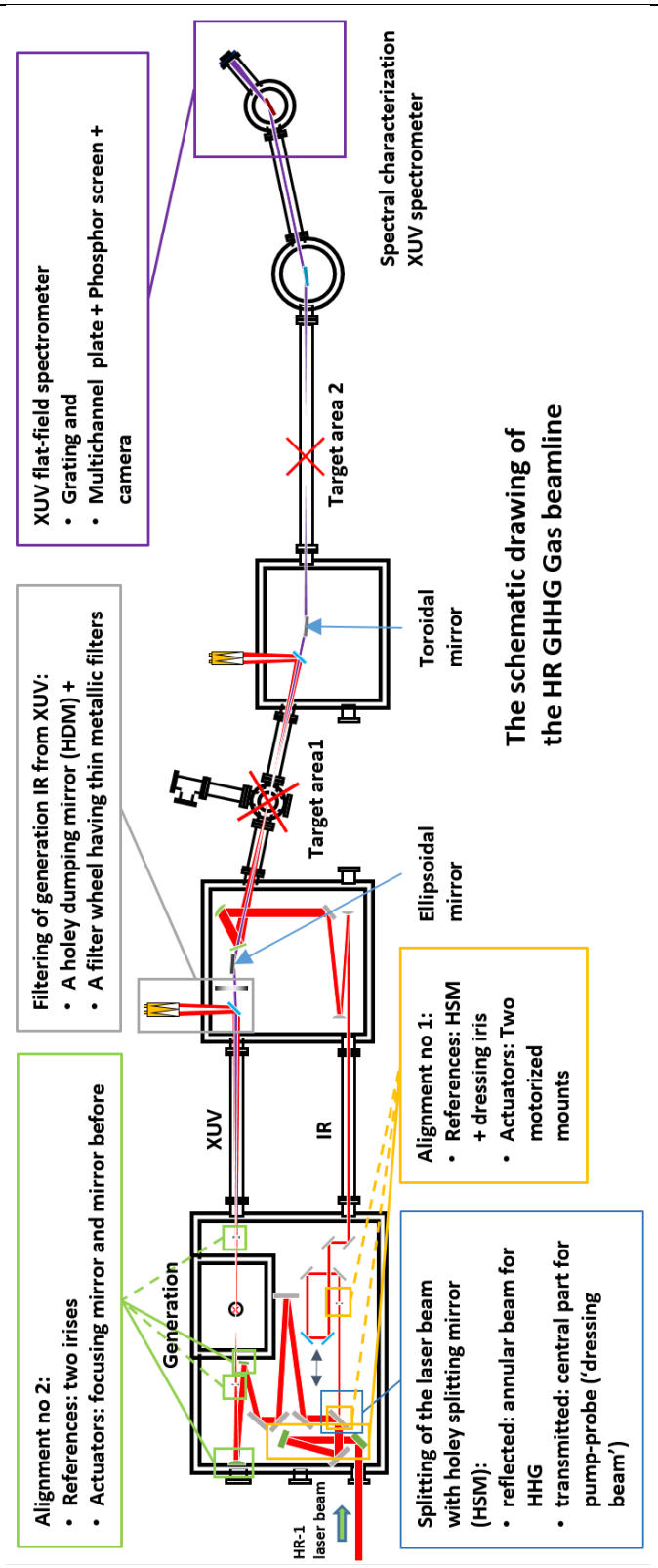

Figure 2. Schematic drawing of the HR GHHG Gas beamline with sections highlighted related to the laboratory practice course.

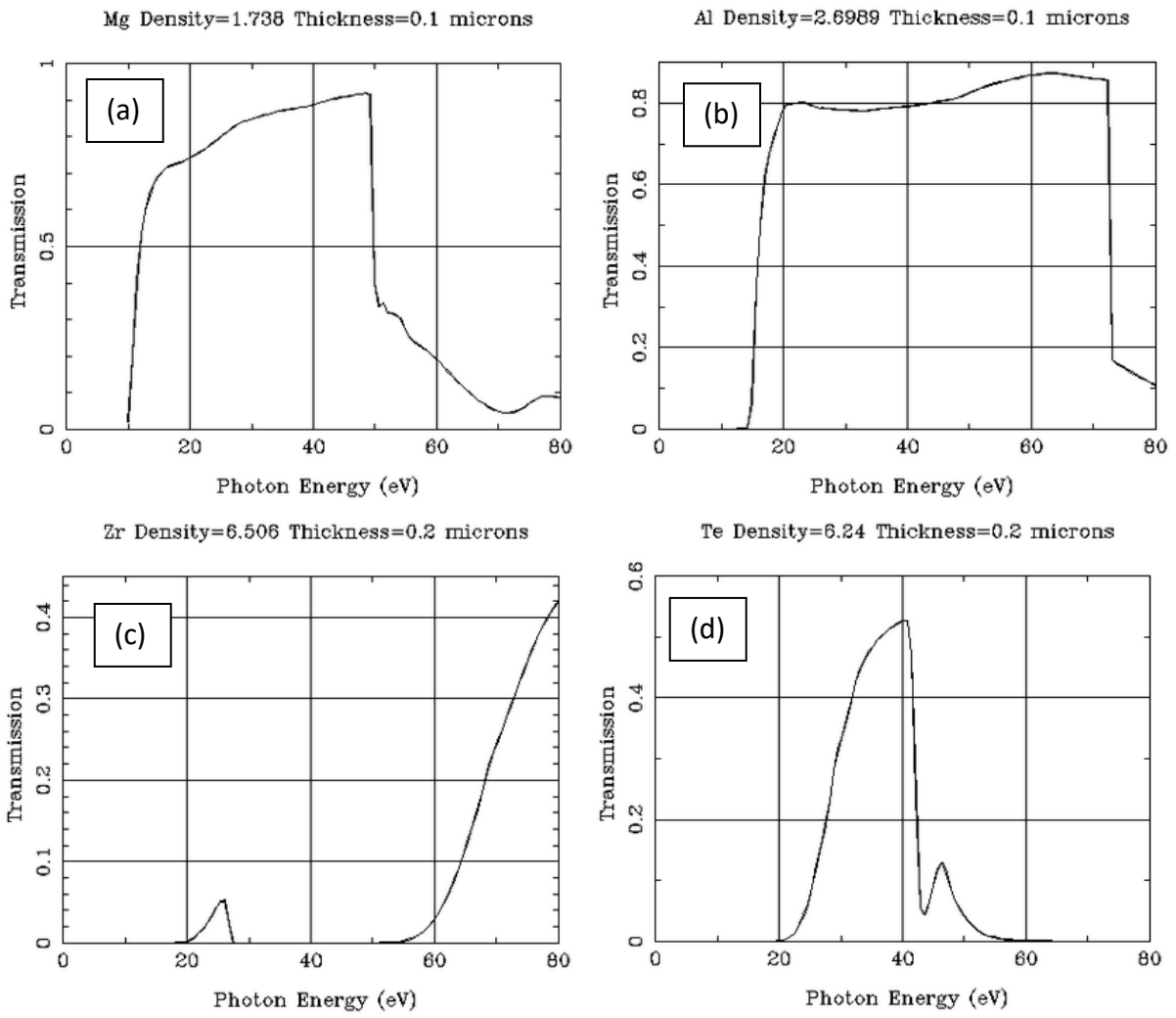

Figure 3. Transmission of thin metallic filters ((a) 100-nm thick magnesium (Mg), (b) 100-nm aluminum (Al), (c) 100-nm zirconium (Zr) and (d) 100-nm tellurium (Te)) in the XUV photon energy range (10 - 80 eV).
The source of data: https://henke.lbl.gov/optical_constants/filter2.html (This link can be used to get transmission data for other materials and other thicknesses in adjustable spectral range.)

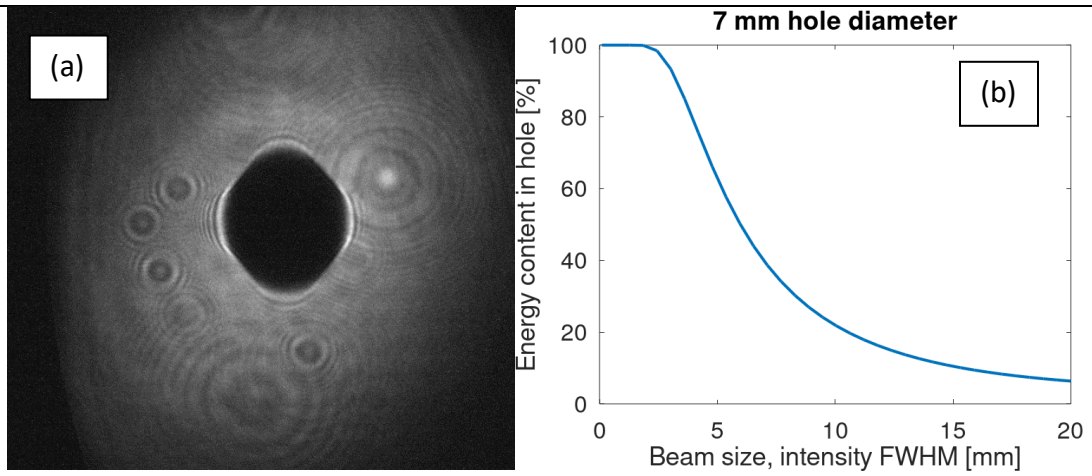

Figure 4. (a) An example image of the beam reflected from the HSM. Note that the hole is not circular because it is oriented 45° with respect to the plane of imaging (see HSM in Fig. 2). Also, diffraction patterns arise due to dust or scattering surfaces on the optics used for imaging the HSM. (b) The energy content of the laser beam within the central hole of the HSM for different beam sizes and a fixed 7 mm hole diameter.

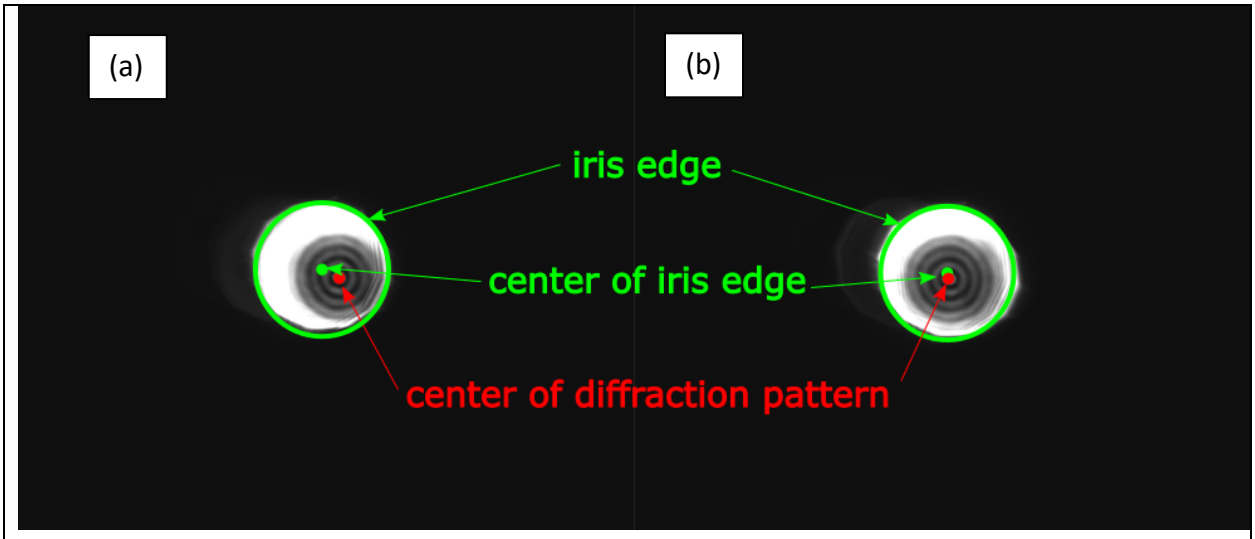

Figure 5. (a) An example camera image showing a misaligned beam since the center of concentric diffraction pattern does not coincide with the center of circle drawn by the iris edge. (b) An example camera image where the beam is almost aligned to the reference.

2.3. Beam steering to experimental area and XUV diagnostics

The XUV beam that is generated during HHG is a beam with a small divergence. Applications of these beams, however need small spot sizes, that is, refocusing or reimaging of the XUV beam. Contrary to the visible or IR wavelength ranges, in the XUV this can only happen with reflective optics, since all materials would absorb the XUV radiation, so no lenses can be used. In addition, since the refractive index of materials in the XUV range are close to unity, relevant reflection can

only happen when total external reflection is used, and this needs grazing incidence (shallow incidence angle with respect to the reflective mirror surface, see Figure 2). Such grazing incidence imaging optics are for example toroidal or ellipsoidal mirrors. The former only allows for imaging with magnification $N = 1$, while ellipsoidal mirrors can be designed to allow for a broad range of magnifications.

In the HR GHHG Gas beamlines the XUV beam in the gas cell is reimaged two times for two interaction regions (see "Target area 1" and "Target area 2" in Figure 2). First, an ellipsoidal mirror is used to focus the beam to "Target area 1" with a magnification of $N_1 = 0.4$, then this reimaged spot is imaged again by a toroidal mirror to target area "Target area 2" with a magnification of $N_2 = 1.0$. After this the XUV beam further propagates towards the XUV diagnostics section (see purple box in Figure 2).

Using simple laws of geometrical optics, the XUV beam size in the gas cell w_{XUV} and the reimaged beam size in target area one relate to each other by

$$N_1 = w_1/w_{\mathrm{XUV}}. \tag{7}$$

It is also known from Gaussian optics that the divergence of the beam is inversely proportional to the beam waist, so the divergence angles θ of the original and reimaged beams are related to each other by

$$N_1 = \theta_{\mathrm{XUV}}/\theta_1. \tag{8}$$

2.4. Spatio-spectral diagnostics of the XUV beam – the flat-field spectrometer (FFS)

To spectrally characterize the generated high-harmonic radiation, in many laboratories flat-field spectrometers are used. In such spectrometers a grating disperses the spectral components of the radiation along one axis, similarly to how it is done the visible range of the electromagnetic spectrum. Thanks to the special design of the grating, a sharp image is formed in a plane where the photo-sensitive detector, a multi-channel plate (MCP) is placed. An example image that is formed on the MCP is shown by Figure 6 (colored image in the middle). In the two-dimensional image the different wavelength components are dispersed along the horizontal axis, while the vertical signal distribution corresponds to the spatial profile of the beam (see Figure (a) and (b)).

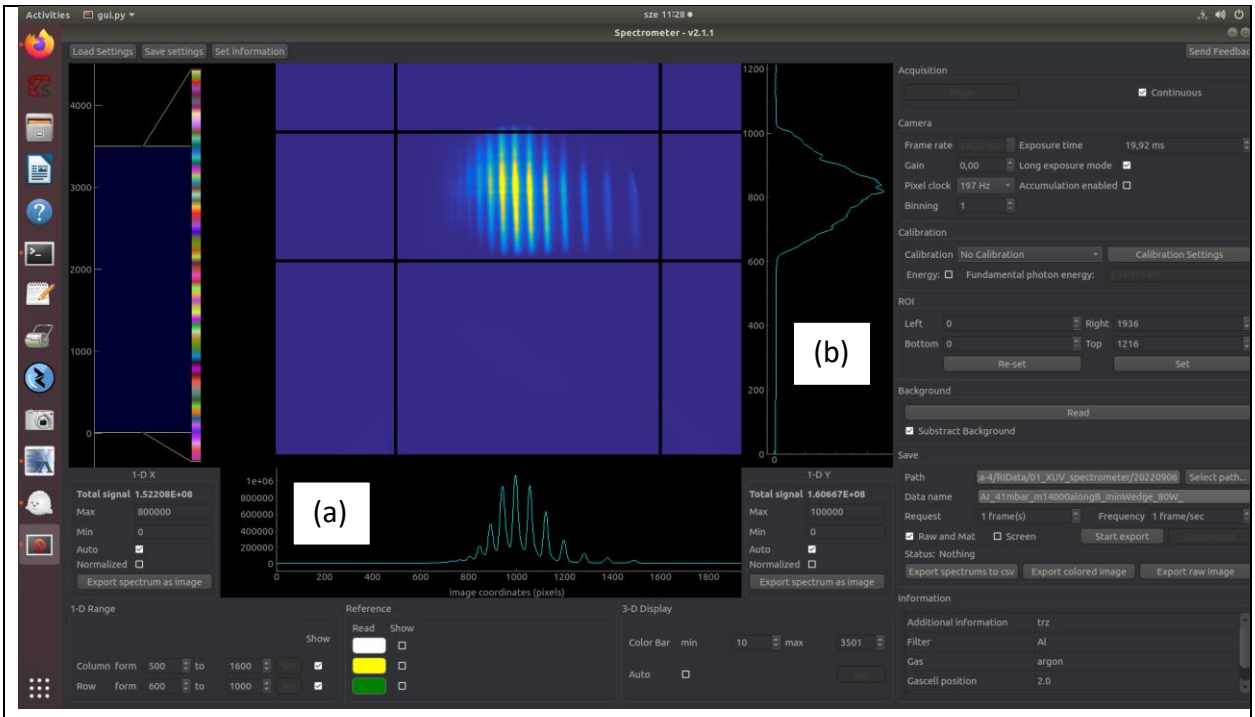

Figure 6. An example image of the software used to save images of the XUV flat-field spectrometer (FFS). (a) A vertical sum of the signal image (colored middle part), showing a spatially integrated harmonic spectrum. (b) A horizontal sum of the signal image (colored middle part), showing a spectrally integrated spatial profile of the XUV beam along the vertical axis.

Unfortunately, XUV FFS are usually not spectrally calibrated, so there is no pre-defined relation between pixel number along the horizontal axis and what wavelength (or photon energy) it corresponds to. Since no golden standard radiation sources exist in this wavelength range for easy calibration, spectral calibration is usually done using the properties of high-harmonics themselves. In the following the basics of this calibration is described. The textbook expression often referred to as “grating equation” is for describing the diffraction angle of radiation having different wavelengths:

$$d \sin\alpha = m\lambda, \tag{9}$$

where d is the slit spacing of the grating, α is the angle of diffraction/reflection, m is the diffraction order and λ is the wavelength of light. Since high-order harmonic peaks have equidistant spacing in frequency (and photon energy, see Figure 1), using the relation

$$E = hf = hc/\lambda, \tag{10}$$

where E is the photon energy, h is the Planck constant, f is the frequency of light, c is the speed of light in vacuum, we rewrite eq. (9) as follows:

$$E = \frac{mhc}{d \sin\alpha}, \tag{11}$$

Using that $\sin\alpha = x/l$, (x being the horizontal pixel coordinate in the detection plane, l the distance of the grating and the detection plane), eq. (11) can be rewritten as

$$E = \frac{mhcl}{d\,x}, \tag{12}$$

which shows that the photon energy of the radiation is inversely proportional to the horizontal pixel coordinate x at which it appears on the detector. Since zero photon energy (infinite diffraction angle) is not within the range of the detector and not all quantities are known in eq. (12), in general the relation of horizontal pixel number and photon energy can be taken in the form

$$E = \frac{a}{x} + b, \tag{13}$$

where a and b are fitting variables. Using that if we are able to identify one harmonic peak (and as a result we know what photon energy corresponds to one certain horizontal pixel in the image), we can identify additional photon energy - pixel relations using that fact that high-order harmonic peaks always have a spacing two times the photon energy of the laser (2x1.2 eV = 2.4 eV spacing of harmonics for the 1030 nm central wavelength of HR-1 laser). By fitting a function of the form of eq. (13) to the photon energies and horizontal pixel numbers identified, one can get what photon energy each horizontal pixel corresponds to (see an example calibration in Figure 7). This is, what is called the spectral calibration of the spectrometer. Identifying a harmonic peak required to do the above is usually done using spectra recorded with and without application of the metallic filter. This will be described in the corresponding task.

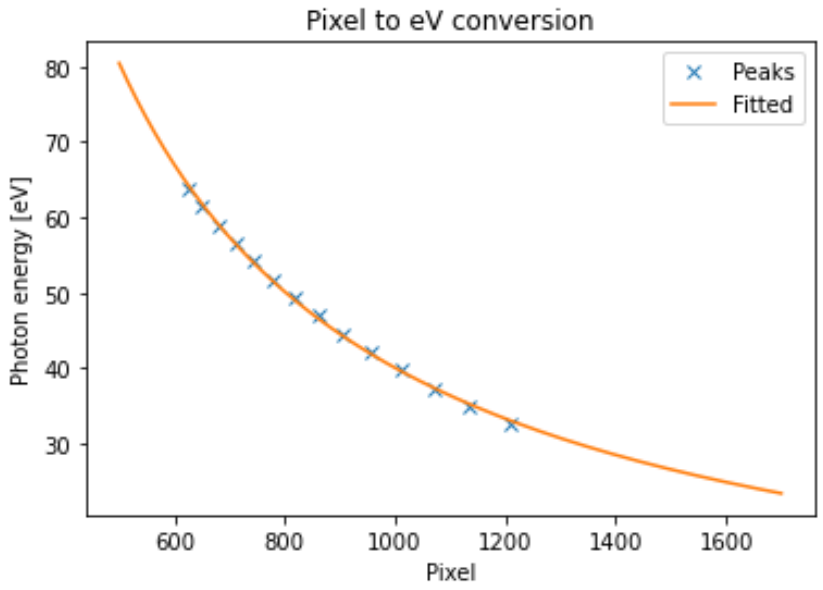

Figure 7. An example horizontal pixel number – photon energy in electronvolt (eV) conversion for calibration of the recorded high-harmonic spectrum. Note: the detector of the FFS is moveable, so this calibration is not necessarily valid for the day of the practice.

3. Practice tasks

3.1. Tasks during the laboratory practice

1. Get acquainted with the safety features of the LTA4 laboratory and the HR GHHG Gas beamline. Sign the attendance sheet.
2. Get an overview of the beamline schematically represented by Figure 2 with the help of the lecturer(s). Identify the different sections of the beamline depicted in Figure 2.
3. Do the alignment of the laser beam (at low laser power) based on the description in Section 2.2 and the instructions of the lecturer(s) for the section called „Alignment no. 1" in Figure 2. Controlling of mirrors and cameras will be described by the lecturer(s).
4. After doing the alignment in the previous point, record an image of the beam reflected by the HSM. Pay attention with camera settings not to saturate the image.
5. Do the alignment of the laser beam (at low laser power) based on the description in Section 2.2 and the instructions of the lecturer(s) for the section called „Alignment no. 2" in Figure 2.
6. Turn on the MCP detector of the FFS spectrometer with the help of the lecturer(s).
7. Start HHG (inject gas into gas cell, switch laser to high power) with the help of the lecturer(s).
8. Record an HHG spectrum using the FFS with having no metallic filter inserted in the beam path.
9. Record an HHG spectrum using the FFS with having a metallic filter (the type of filter will be given by the lecturer(s)) inserted in the beam path.
10. Participate to shutting down the beamline.

3.2. Tasks for measurement report preparation

11. Estimate the peak intensity in the laser focus of the HR GHHG Gas beamline (using eqs (5) and (6)). **Use the following parameters: central wavelength $\lambda = 1030\ \mathrm{nm}$, pulse energy $\varepsilon_n = 1\ \mathrm{mJ}$ and pulse duration $\tau = 40\ \mathrm{fs}$ and focal length $\mathrm{f} = 90\ \mathrm{cm}$.** For estimating the input beam size w_{in}, use the beam profile recorded at the HSM (see Task no. 4). To estimate the beam size, fit a Gaussian function of the form

$$I(x) = A \exp\left(-\frac{2(x - x_0)^2}{w_{\mathrm{in}}^2}\right) + B \tag{14}$$

to a vertical lineout of the recorded image (see Figure 8 for example). During evaluation, consider that the data points in the hole have to be disregarded! For calibration of the pixel size – real size, consider that the hole diameter is known (7 mm). Give an estimation for the peak intensity considering also the energy loss in the hole using the plot of Figure 4(b).

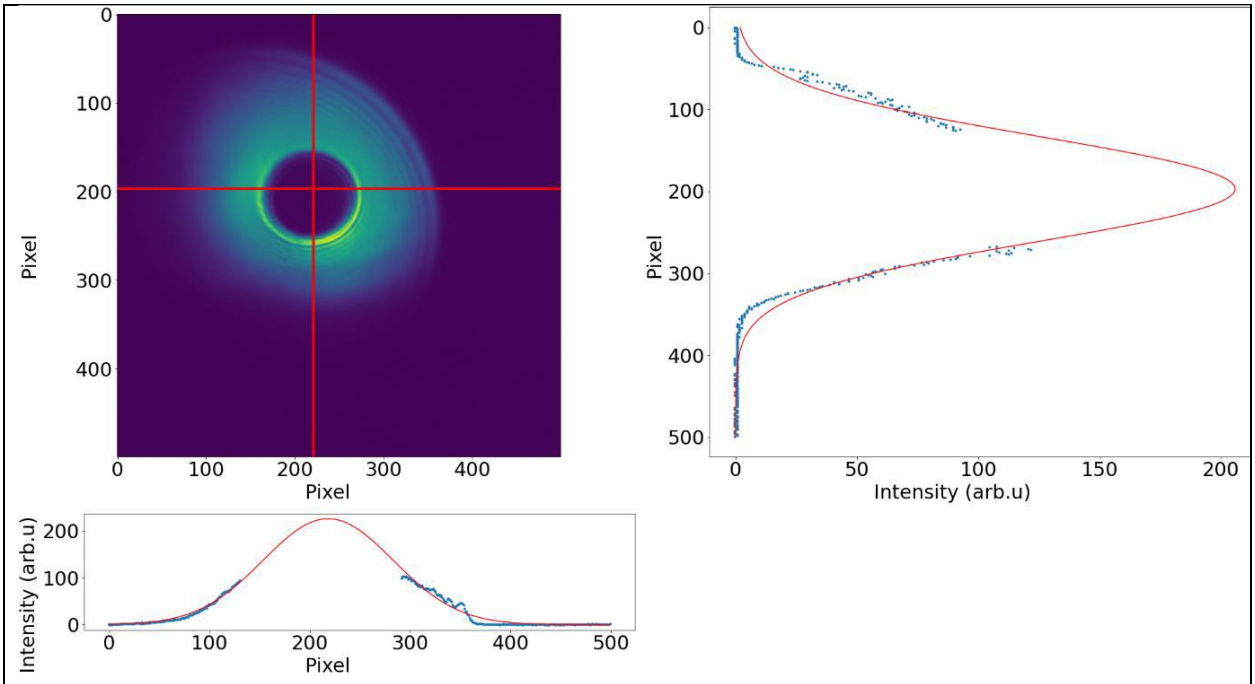

Figure 8. An example of fitting a Gaussian profile to the recorded HSM image.

12. Estimate the microscopic cut-off (using eqs. (1) and (3)) based on the intensities obtained in the previous task (Task 11) and the gas used for generation. Do the estimation for both cases (considering and not considering the energy loss in the hole).
13. Calibrate the XUV FFS images based on the description in Section 2.4. Use the two FFS images recorded during Task 8 and 9. To identify the single harmonic necessary as a first step for calibration, divide the spatially integrated images taken with and without filter. This will give you a curve where the sharp absorption edge of the specific filter can be recognized, allowing you to identify neighboring harmonic peaks. Plot the calibrated spectra along with the filter transmission curve, similarly to Figure 9. For theoretical filter transmission use the link in the caption of Figure 3.

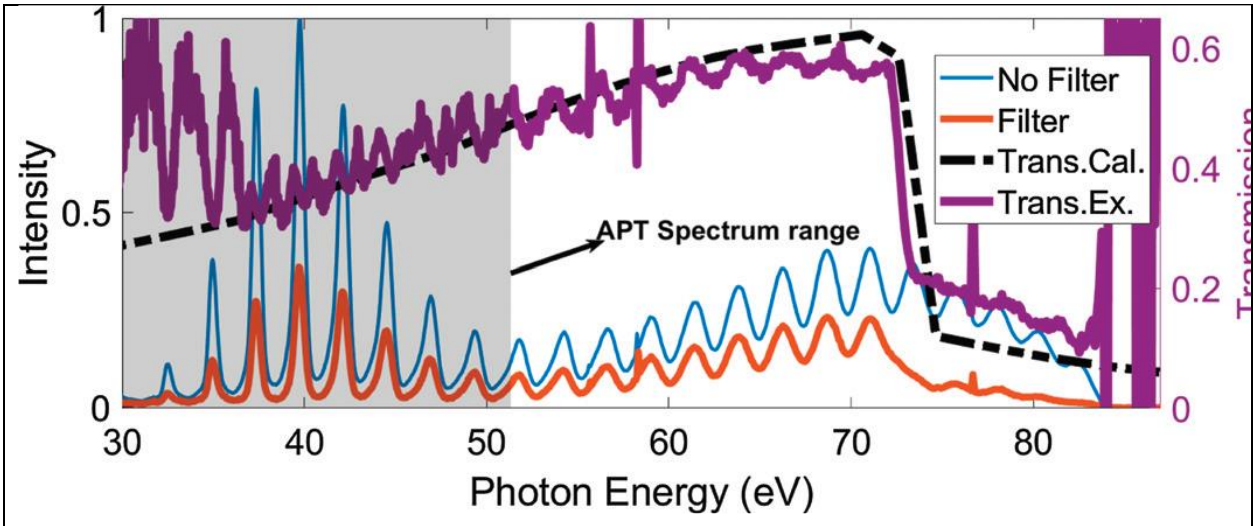

Figure 9. Calibrated XUV spectra and filter transmission curves showing the spectrum recorded without filter (curve "No filter"), with filter (curve "Filter"), the theoretically ("Trans. Cal.") experimentally obtained transmission curves ("Trans ex.").

14. Based on the calibrated XUV spectrum without filter obtained in the previous task, give the macroscopically obtained cut-off. How does it relate to the microscopic cut-off estimation from Task 12? What could be the source of the difference?
15. Sum the XUV spectrum recorded without filter along the spectral axis (see example in Figure 6(b)). Fit a Gaussian function of the form of eq. (12) to estimate the beam size at the detector plane **(w_2). For the calibration of pixel number to physical size similarly to task 11, use that the smaller side of the FFS image (the vertical one with 1296 pixel) corresponds to 40 mm distance.** Use this to calculate the divergence of the beam in „Target area 2" using the formula

$$\theta_{\mathrm{XUV}} = w_2/D, \tag{15}$$

Where $D = 2.5\ m$ is the distance of „Target area 2" and the detection plane.

16. Estimate the beam divergence θ_{XUV} of the XUV beam originating from the gas cell using the description in Section 2.3. Consider that reimaging happens two times from the gas cell to the FFS detection plane!
17. Estimate the divergence of the IR beam using eq. (15) using the input beam size w_{in} in Task 11 and the focal length of the focusing optics. How do the divergences of the XUV and IR fields relate to each other? Does it fit the theoretical prediction?

4. Entry/control questions

- Write down the cut-off law of HHG and explain the meaning of quantities present in it!

- How does the XUV beam size and divergence relate to the same properties of the focused laser beam used for HHG?
- What else defines the observable HHG spectrum other than the cut-off law of the simple man's model?
- What three laser parameters does the peak intensity of the focused laser beam depend on?
- Why do HHG experiment have to be done in vacuum?
- Why grazing incidence reflective optics are necessary for XUV beam steering?

5. References

[1] Zenghu Chang, "Fundamentals of Attosecond Optics", CRC Press, 2016

[2] Peng Ye et al., J. Phys. B: At. Mol. Opt. Phys. 53 154004 (2020)